Hepatocellular Shuttling and Recirculation of Sorafenib-Glucuronide is Dependent on Abcc2, Abcc3, and Oatp1a/1b

Aksana Vasilyeva[1,*], **Selvi Durmus**[2,*], **Lie Li**[1], **Els Wagenaar**[2], **Shuiying Hu**[1], **Alice A. Gibson**[1], **John C. Panetta**[1], **Sridhar Mani**[3], **Alex Sparreboom**[1], **Sharyn D. Baker**[1], and **Alfred H. Schinkel**[2]

[1]Department of Pharmaceutical Sciences, St. Jude Children's Research Hospital, Memphis, Tennessee [2]Division of Molecular Oncology, The Netherlands Cancer Institute, Amsterdam, The Netherlands [3]Department of Medicine, Albert Einstein College of Medicine, Bronx, New York

Abstract

Recently, an efficient liver detoxification process dubbed 'hepatocyte hopping' was proposed based on findings with the endogenous compound, bilirubin glucuronide. According to this model, hepatocytic bilirubin glucuronide can follow a liver-to-blood shuttling loop via Abcc3 transporter-mediated efflux and subsequent Oatp1a/1b-mediated liver uptake. We hypothesized that glucuronide conjugates of xenobiotics, such as the anticancer drug sorafenib, can also undergo hepatocyte hopping. Using transporter-deficient mouse models, we show here that sorafenib-glucuronide can be extruded from hepatocytes into the bile by Abcc2 or back into the systemic circulation by Abcc3, and that it can be taken up efficiently again into neighboring hepatocytes by Oatp1a/1b. We further demonstrate that sorafenib-glucuronide excreted into the gut lumen can be cleaved by microbial enzymes to sorafenib which is then reabsorbed, supporting its persistence in the systemic circulation. Our results suggest broad relevance of a hepatocyte shuttling process known as "hepatocyte hopping" – a novel concept in clinical pharmacology - for detoxification of targeted cancer drugs which undergo hepatic glucuronidation, such as sorafenib.

Keywords

Sorafenib; hepatocyte; glucuronidation; transport; recirculation

INTRODUCTION

Sorafenib is a multi-kinase inhibitor that is approved for treatment of advanced thyroid (1), renal cell (2), and hepatocellular carcinomas (3), and is being evaluated for treatment of acute myeloid leukemia (4), and ovarian cancer (5). Like other orally-administered tyrosine kinase inhibitors, sorafenib displays wide interindividual pharmacokinetic variability, which can significantly affect drug-induced toxicity and possibly efficacy (6, 7). Although the metabolic pathways of sorafenib have been reasonably well established, involving a CYP3A4-mediated route to form sorafenib-N-oxide (8) and a UGT1A9-mediated route to form sorafenib-glucuronide (SG) (9), the primary causes of the pharmacokinetic variability remain unknown (10, 11). It has been suggested that sorafenib undergoes enterohepatic recirculation, a process that involves removal of solutes from blood by uptake into hepatocytes, excretion into bile, and intestinal reabsorption, sometimes accompanied by hepatic conjugation and intestinal deconjugation (12). However, the occurrence of enterohepatic recirculation of sorafenib has not been experimentally demonstrated but was inferred from *in vitro* biliary clearance studies in sandwich-cultured human hepatocytes (13), and provides a means to explain observed time profiles of sorafenib levels in plasma of cancer patients (14).

We recently reported that mice lacking 1A- and 1B-type organic anion-transporting polypeptides (Oatp1a/1b), uptake transporters localized to the sinusoidal (basolateral) membrane of hepatocytes, experience substantially increased plasma levels of SG after oral sorafenib administration (15). This phenomenon resembles our earlier findings with conjugated bilirubin (16, 17), whereby Oatp1a/1b-deficiency leads to excessive buildup of bilirubin-glucuronide (BG) in the systemic circulation, which can ultimately result in jaundice. In the case of bilirubin, Oatp1a/1b transporters work in concert with the basolaterally located efflux transporter Abcc3 (Mrp3) to mediate hepatic efflux and subsequent reuptake of BG into hepatocytes, a phenomenon we called 'hepatocyte hopping' (16, 18). This process is operational not only under pathological, but also normal physiological conditions, and results in a substantial amount of hepatocytic BG not being secreted into bile by Abcc2 (Mrp2), but transported back into the blood by Abcc3. These molecules are then taken up again in adjacent downstream hepatocytes by Oatp1a/1b, affording another chance of being secreted into bile. This liver-to-blood shuttling loop allows management of situations where biliary secretion in upstream hepatocytes is saturated, for example due to substrate overload or incidental inhibition (18). With this process, BG can be safely eliminated, instead of becoming trapped inside upstream hepatocytes. Thus, a more evenly distributed biliary secretion of substrates over the entire liver lobule can be achieved, leading to an efficient hepatic detoxification. Although demonstrated so far only for one endogenous solute, based on the broad substrate specificity of the transporters involved (19), it is possible that many xenobiotics and their glucuronide conjugates are subject to the same hepatocyte hopping process.

In the current study, we aimed to understand the processes underlying sorafenib glucuronide hepatocyte shuttling, biliary excretion, and intestinal recycling using *in vitro* and *in vivo*

models, and thus to elucidate mechanisms contributing to sorafenib interindividual pharmacokinetic variability.

MATERIALS AND METHODS

In vitro vesicular transport

Vesicles from Sf9 cells (Life Technologies) expressing mouse Abcc2 (mAbcc2), rat Abcc2 (rAbcc2), human ABCC2 (ABCC2), human ABCC3 (ABCC3), or human ABCC4 (ABCC4) were incubated with sorafenib (10 μM; Chemie Tek, Indianapolis, IN) or SG (10 μM) for 5 min in the presence or absence of ATP (4 mM) or rifampin (100 μM), then lysed with 0.1 M HCl, and analyzed by liquid chromatography-tandem mass spectrometry (LC-MS/MS) (20). ATP-dependent transport of sorafenib and SG was determined by subtracting AMP-dependent transport from ATP-dependent transport, with both expressed in pmol/min/mg, after normalization for non-specific transport observed in control vesicles. Uptake experiments were carried out at a concentration of 10 μM, which is equivalent to average sorafenib plasma steady-state concentrations achievable in adults and children treated at 400 mg or 200 mg/m^2 twice daily (9, 21).

Animals

Abcc4(−/−) mice on a C57BL/6 background were generated and bred in-house at St. Jude Children's Research Hospital, and Abcc2(−/−) mice on an FVB background were provided by Taconic (Hudson, USA). All other knockout strains on an FVB background were generated and bred in-house at The Netherlands Cancer Institute. Real-time PCR analyses demonstrated that the expression of relevant drug transporters did not substantially change in any of these knockout strains (Supplementary Table S1). Therefore, the possibility of major compensatory changes in transporter expression affecting the interpretation of results was ruled out. Abcc2(−/−) rats on a Sprague-Dawley background were obtained from Sage Labs. Mice and rats were housed in a temperature-controlled environment with a 12-hour light cycle and given a standard diet and water *ad libitum*. Experiments were approved by the Institutional Animal Care and Use Committees of St. Jude Children's Research Hospital and the Netherlands Cancer Institute.

Plasma pharmacokinetic studies

Murine studies were performed as described (15). Briefly, mice were fasted for 3 hours prior to administration of sorafenib (10 mg/kg; formulated in 50% Cremophor EL and 50% ethanol, then diluted 1:4 with deionized water) by oral gavage. A sorafenib dose of 10 mg/kg in FVB wildtype mice achieves sorafenib plasma steady-state concentrations ranging from ~ 6 to 10 μM, similar to that achieved in humans. Serial blood samples were taken from individual mice at 0.25, 0.5, and 1 hour from the submandibular vein, at 2 and 4 hours from the retro-orbital sinus and at 7.5 hours by a terminal cardiac puncture (Abcc2(−/−) and Abcc4(−/−) mice); or by tail vein sampling at 0.25, 0.5, 1, 2 and 4 hours and at 8 hours by a terminal cardiac puncture (all other knockout strains). In Oatp1a/1b(−/−) mice and all other double- and triple-knockout mice, serial tail vein blood samples were obtained at 0.25, 0.5, 1, and 2 hours (~peak concentration) after drug administration, and livers were obtained at the last time point. To evaluate the role of enterohepatic cycling in sorafenib disposition,

FVB wildtype mice received neomycin (200 mg/kg; diluted in saline) by oral gavage, every 12 hours for 5 days. On the last day, mice received SG (10 mg/kg diluted in water) immediately after the last neomycin dose. In an initial study, serial blood samples were taken from individual mice at 0.25, 1, 2, 4, 8 and 24 hours after SG administration, and sorafenib was not detected in plasma until 8 hours after SG administration. In a follow-up study, SG was administered and serial blood samples were obtained at 8 (submandibular vein), 12 and 16 hours (retro-orbital sinus), and at 24 hours (cardiac puncture). For studies with rats, animals were fasted overnight before administration of sorafenib (10 mg/kg), and serial blood samples were taken at 0.5 and 1.5 hours (retro-orbital plexus), 4 and 8 hours (saphenous vein), 12 hours (tail vein), and 24 hours (cardiac puncture). All blood samples were centrifuged at 3,000×g for 5 min, and tissues were homogenized in 10 volumes (w/v) of water and stored at −80°C until analysis. Sorafenib and SG pharmacokinetic parameters in all mouse strains were calculated using noncompartmental techniques via WinNonlin 6.3 (Pharsight). In addition, sorafenib plasma concentration-time data from wildtype and Abcc2(−/−) mice were analyzed simultaneously using population pharmacokinetic modeling via Monolix version 4.3.3. (22). A one-compartment model with first-order oral absorption was used to model the data. A covariate (wildtype versus knockout mouse) on a single parameter was considered significant if the -2 Log-Likelihood was decreased by at least 3.84 units (P<0.05).

Urinary excretion studies

Mice were placed into metabolic cages at least 3 days prior to the start of the study and were kept on reverse 12-hour light cycle, with free access to a standard diet and water *ad libitum*. After mice received a single dose of sorafenib (10 mg/kg) by oral gavage, serial blood samples were taken at 4.5, 24, 48, and 72 hours and plasma was isolated by centrifugation. Urine was collected for 72 hours after sorafenib administration. Plasma, urine, and liver concentrations of sorafenib, sorafenib-N-oxide, and SG were determined by liquid chromatography-tandem mass spectrometry.

Bile collection

Bile duct cannulation/catheterization was done as described (23), except that animals remained under isoflurane anesthesia during the surgery and bile collection. For studies in mice, bile collection was started 30 minutes after oral sorafenib administration and continued for 2 hours. In rats, bile collection was started 2.5 hours after oral sorafenib administration and continued for 2 hours, using 15-min fractions.

Ex vivo microsomal incubations

Mouse liver and intestinal microsomes were prepared as described (24, 25), and rat liver microsomes were purchased from Sigma-Aldrich. Incubations were performed as described (9).

Ex vivo cecal incubations

Cecal contents were extracted from euthanized mice, divided into equal parts, and immediately placed into 4-ml thioglycollate media. In select experiments, enzymatic activity

was terminated by heat (65°C) pre-treatment for 30 min. Incubations were initiated by addition of SG (2 μM), and formation of sorafenib was assessed in serial 50-μl aliquots obtained at 0, 0.25, 0.5, 1, 3, and 6 hours.

Statistical analysis

All data shown are mean ± SE. Statistical analyses were done using GraphPad Prism 5.0. All tests were 2-tailed t-tests, and P<0.05 was considered statistically significant.

RESULTS AND DISCUSSION

Identification of SG as a substrate of ABCC2, ABCC3, and ABCC4

In order to identify efflux proteins involved in the transport of sorafenib and SG in hepatocytes, experiments were initially carried out using inside-out vesicles expressing various transporters of the ABCC family. Following a 5-min incubation period, sorafenib uptake was moderately increased by human ABCC2, but not by ABCC3, ABCC4 or mouse Abcc2 (Fig. 1A). Rat Abcc2 may also transport sorafenib, albeit weakly. The modest transport of sorafenib by human ABCC2 is consistent with an earlier report demonstrating that overexpression of ABCC2 results in resistance to sorafenib-induced cell growth inhibition (26).

Unlike for sorafenib, uptake of SG was efficiently increased relative to control vesicles by each transporter tested (Fig. 1B). ABCC2-, ABCC3- and ABCC4-mediated uptake was sensitive to inhibition by rifampin (Fig. 1B), a known inhibitor of ABCC (27). The transport of SG by human ABCC2 was saturable with a Michaelis-Menten constant (Km) of 22 ± 6.6 μM and a maximal velocity (Vmax) of 155 ± 11 pmol/min/mg, corresponding to a value for transport efficiency (Vmax/Km) of 7.0 (Fig. 1C). The transport of SG by ABCC3 (Km, 186 ± 72 μM; Vmax, 196 ± 44 pmol/min/mg) and ABCC4 (Km, 146 ± 14 μM; Vmax, 221 ± 11 pmol/min/mg) was also saturable (Fig. 2D-E), but the transport efficiency was about 7-fold lower than that observed for ABCC2.

ABCC2 mediates biliary excretion of SG

The *in vivo* role of ABCC2 in the transport of sorafenib and SG was next evaluated in Abcc2-deficient [Abcc2(−/−)] mice receiving oral sorafenib (Supplementary Table S2). Compared to wildtype mice, Abcc2-deficiency was not associated with altered plasma disposition of sorafenib (Fig. 2A), liver uptake (Fig. 2B, Supplementary Fig. S1A),or biliary output (Fig. 2C, Supplementary Fig. S1C). In contrast, plasma levels of SG after sorafenib administration were increased by ~350-fold in Abcc2(−/−) mice (Fig. 2D), and accompanied by a decreased liver-to-plasma ratio, and ~3-fold increase in liver concentrations (Fig. 2E; Supplementary Fig. S1B). These changes were not due to increased hepatic or intestinal biotransformation of sorafenib (Supplementary Fig. S2A and B) or to shunted urinary excretion, which was found to be a minor route of elimination irrespective of Abcc2 status (Supplementary Fig. S2C and D). Consistent with the known localization of Abcc2 on the bile canalicular membrane (28), we found that the biliary output of SG was reduced by ~12-fold in Abcc2(−/−) mice (Fig. 2F; Supplementary Fig. S1D), in spite of a ~3-fold higher liver concentration. These findings suggest that under Abcc2-proficient conditions, SG is

effectively secreted into bile and its appearance in the systemic circulation represents an overshoot mechanism that poorly reflects the extent of its formation (29).

To determine whether these phenotypes are also observed in another species, sorafenib pharmacokinetics were assessed in wildtype and Abcc2(−/−) rats. Abcc2-deficiency in rats resulted in a ~2-fold increase in plasma levels of both sorafenib (Fig. 3A) and sorafenib-N-oxide (Fig. 3B). Unexpectedly, however, SG was not detected in plasma or bile of either wildtype or Abcc2(−/−) rats (Fig. 3C). *Ex vivo* metabolism studies indicated that, compared to mice and humans (9), rat liver microsomes lack a significant capacity to form SG (Fig. 3D). These results indicate that the rat is an inadequate model for the human pharmacokinetics of sorafenib. Moreover, the involvement of ABCC2 in the transport of unchanged sorafenib may become increasingly important when glucuronidation is defective, a possibility that is consistent with recent clinical data (10). Collectively, the data indicate that biliary excretion of SG is primarily mediated by ABCC2 and therefore is an important determinant of SG pharmacokinetics.

Oatp1a/1b and Abcc3 transporters cooperatively transport SG *in vivo*

The disposition of sorafenib was next evaluated in wildtype, Oatp1a/1b(−/−), Abcc3(−/−), and Oatp1a/1b;Abcc3(−/−) mice. Plasma levels of sorafenib were not substantially altered in any of the strains (Supplementary Fig. S3A), and liver levels of sorafenib were also similar between knockout and wildtype strains (Supplementary Fig. S3B), although plasma sorafenib exposure was ~25% lower in Oatp1a/1b(−/−) mice, similar to our previous observations (15). These findings indicate that the differences between the strains were marginal for plasma and liver levels of sorafenib, and unlikely to directly confound the interpretation of SG levels.

As shown previously (15), the impact of Oatp1a/1b transporters on the disposition of SG was far higher than that for sorafenib, and absence of the Oatp1a/1b transporters resulted in a ~60-fold increase in the plasma levels of SG (Fig. 4A; Supplementary Table S2). Importantly, this increase was partially reversed (by ~2-fold) in Oatp1a/1b;Abcc3(−/−) mice, suggesting that Abcc3 activity contributes to the increased plasma levels of SG. In contrast, Abcc3 deficiency alone did not lead to altered plasma SG levels, indicating that the impact of Abcc3 does not come to the fore in the presence of Oatp1a/1b transporters (Fig. 4A). Similar results were obtained in a separate experiment terminated at 2 hours (i.e., around the peak plasma levels of SG), showing 125- and 56-fold increased plasma levels in Oatp1a/1b(−/−) and Oatp1a/1b;Abcc3(−/−) mice compared to wildtype mice, respectively (Supplementary Table S3). In liver samples, there was only a slight increase in SG levels in both Oatp1a/1b(−/−) and Oatp1a/1b;Abcc3(−/−) mice compared to the wildtype strain (Fig. 4B), and an accordingly large decrease in liver-to-plasma ratio (Fig. 4C). As might be expected, in both Abcc3-deficient strains, liver-to-plasma ratios of SG were somewhat increased relative to their Abcc3-proficient counterparts (Fig. 4C). These data suggest a major role of Oatp1a/1b transporters in hepatic (re-)uptake of SG and a clear impact of Abcc3 on sinusoidal extrusion of SG. The role of Abcc3 as a hepatic basolateral efflux transporter of SG is consistent with the previous observation that SG can be extruded into

the medium of sandwich-cultured hepatocytes exposed to sorafenib (13), and with its partial recovery in urine of patients treated with sorafenib (29).

Since the present results indicate the presence of another efflux transporter located at the sinusoidal membrane of hepatocytes that can mostly compensate for the loss of Abcc3, we next evaluated whether Abcc4 could be this partially redundant transporter. Using Abcc4(−/−) and Abcc3;Abcc4(−/−) mice, we found that concentrations of SG in plasma and liver were not substantially affected by Abcc4 deficiency, whereas Abcc3(−/−) and Abcc3;Abcc4(−/−) mice did show increased SG liver-to-plasma concentration ratios compared to both other strains (Supplementary Fig. S4; Supplementary Table S3). Similar observations were made for single Abcc4-deficiency in another mouse strain, C57BL/6 (Supplementary Table S2). The data indicate that Abcc4 deficiency, unlike Abcc3 deficiency, does not have a noticeable impact on the sinusoidal efflux of SG *in vivo*. The effective expression of mouse Abcc4 in the sinusoidal membrane may be too low to exert much effect. Moreover, the modest effect of the Abcc3 deficiency in reducing plasma SG levels in Oatp1a/1b/Abcc3(−/−) and in Oatp1a/1b/Abcc2/Abcc3(−/−) mice (Fig. 4A and 4D) suggests that there are one or more other sinusoidal SG efflux mechanisms of unknown identity, that may provide about similar SG efflux activity as the sinusoidal Abcc3.

Sinusoidal transport of SG is affected by Abcc2 and Abcc3 deficiency

The disposition of sorafenib was then evaluated in Oatp1a/1b;Abcc2(−/−), and Oatp1a/1b;Abcc2;Abcc3(−/−) mice. In line with our findings in the single Abcc2(−/−) mice, we found that deletion of Abcc2 in combination with deletion of Oatp1a/1b led to a very large increase in plasma exposure of SG compared to wildtype mice (909-fold), but also compared to Oatp1a/1b(−/−) mice (12.7-fold) (Fig. 4D; Supplementary Table S2). At 2 hours, the liver levels of SG were 1.8-fold higher in the Oatp1a/1b;Abcc2(−/−) mice compared to wildtype mice (Fig. 4E). As a result of the highly increased plasma levels of SG, liver-to-plasma ratios decreased in all transporter knockout mice compared to wildtype mice (Fig. 4F). These findings support an important role for Abcc2 in the biliary excretion of SG, and that deletion of Abcc2 in addition to Oatp1a/1b-deficiency leads to a major increase in the sinusoidal extrusion of this metabolite back into the circulation.

We found that SG plasma exposure was reduced by 30% in Oatp1a/1b;Abcc2;Abcc3(−/−) mice compared to Oatp1a/1b;Abcc2(−/−) mice (Fig. 4D). The impact of Abcc3 in liver remained noticeable with a 1.5-fold increase in absolute levels of SG in liver (Fig. 4E) and a 1.7-fold increase in the liver-to-plasma ratios (Fig. 4F) at 2 hours in Oatp1a/1b;Abcc2;Abcc3(−/−) mice compared to Oatp1a/1b;Abcc2(−/−) mice. Plasma and liver levels of sorafenib were not substantially altered in these strains (Supplementary Fig. S3C-D). Collectively, these findings indicate that Abcc3 has a clear impact on sinusoidal secretion of SG, and in combination with the previously demonstrated ability of Oatp1a/1b to take up SG across the sinusoidal membrane, can result in "hepatocyte hopping" of this drug conjugate. However, there are other partially redundant sinusoidal efflux transporters for SG which limit the absolute impact of Abcc3 deficiency in mice, perhaps especially at the high hepatocyte SG levels caused by the impaired biliary excretion via Abcc2.

SG deconjugation by mouse intestinal β-glucuronidases

In order to assess the fate of SG secreted by Abcc2 into bile, we next performed *ex vivo* incubation studies of mouse intestinal (cecal) content based on the consideration that once in the intestines, SG may serve as a substrate for bacterial β-glucuronidase enzymes that are produced by bacteria normally inhabiting the intestines (30). The removal of the glucuronide group in SG by β-glucuronidase generates a carbon source for the bacteria and, in the process SG is reactivated back to the pharmacologically active sorafenib. Over a 6-hour period in a crude suspension of cecal content, we observed a time-dependent decrease in SG levels and a corresponding increase in sorafenib (Fig. 5A). Heat-pretreatment of the cecal samples at 65°C resulted in abrogation of sorafenib formation, indicating that the deconjugation of SG is an enzyme-mediated process. Furthermore, we found that the formation of sorafenib from SG was reduced by ~3-fold in cecal samples from mice that had been pretreated with neomycin to eliminate the intestinal flora (31) (Fig. 5B). This finding is consistent with the conjecture that β-glucuronidases produced by intestinal microbiota are responsible for the deconjugation of SG to sorafenib.

To demonstrate that sorafenib can be generated from SG *in vivo*, wildtype mice received neomycin or vehicle for 5 days followed by oral administration of a single dose of SG. In an initial study, highly variable peak SG concentrations (15.4 – 3788 ng/mL) were observed at 15 minutes with rapid elimination within 1 to 2 hours, but sorafenib was not detected in plasma until 8 hours after SG administration. In a repeat study, blood was collected more frequently between 8 and 24 hours. Whereas sorafenib levels in plasma of neomycin-pretreated mice were below the limit of quantification, significant levels of sorafenib in plasma were observed in vehicle-pretreated mice, with a delay in peak levels (226–897 ng/mL) at 8 hours after SG administration (Fig. 5C). The substantial delay in availability of sorafenib from SG de-conjugated in the small intestine of mice suggests that an 8-hour sample collection period is too short to observe effects of strongly altered SG disposition in transporter-deficient mice on parent drug levels in plasma following sorafenib administration (Fig. 2, Supplementary Figs. S3 and S5). Nonetheless, these results illustrate the principle that SG biliary excretion followed by intestinal de-glucuronidation may contribute to extended maintenance of sorafenib plasma exposure in humans, and are consistent with the recent observation that neomycin treatment in humans decreased systemic exposure to sorafenib by more than 50% (32). In follow-up studies it will be of interest, based on a physiologically-based pharmacokinetic model for sorafenib, to confirm this concept in Oatp1a/1b- and Abcc2-deficient mice employing repeat dosing regimens.

In conclusion, this study shows that a sinusoidal liver-to-blood shuttling loop for SG is formed by Oatp1a/1b, Abcc3 and likely another sinusoidal efflux transporter. Thus, in addition to endobiotic glucuronide metabolites like BG, xenobiotics that undergo hepatic glucuronidation can also be subject to the same hepatocyte hopping process, depending on the relative affinity of these compounds for sinusoidal and canalicular efflux transporters, such as Abcc2 (Fig. 6). Given the broad substrate specificity of these transporters, we expect that our findings will have relevance for many other xenobiotic glucuronides. These findings also suggest that factors that interfere with the hepatocellular shuttling, biliary excretion and/or intestinal deconjugation of SG will have a major impact on sorafenib systemic

exposure and likely contribute to the substantial interindividual pharmacokinetic variability observed with sorafenib and other tyrosine kinase inhibitors undergoing glucuronidation and enterohepatic recirculation, such as regorafenib (33).

Supplementary Material

Refer to Web version on PubMed Central for supplementary material.

Acknowledgment

We thank Dr. John D. Schuetz for providing the C57BL/6 Abcc4(−/−) mice.

References

1. Gild ML, Bullock M, Robinson BG, Clifton-Bligh R. Multikinase inhibitors: a new option for the treatment of thyroid cancer. Nat Rev Endocrinol. 2011; 7:617–624. [PubMed: 21862995]

2. Iacovelli R, Alesini D, Palazzo A, Trenta P, Santoni M, De Marchis L, et al. Targeted therapies and complete responses in first line treatment of metastatic renal cell carcinoma. A meta-analysis of published trials. Cancer Treat Rev. 2014; 40:271–275. [PubMed: 24070900]

3. Abdel-Rahman O, Fouad M. Sorafenib-based combination as a first line treatment for advanced hepatocellular carcinoma: A systematic review of the literature. Crit Rev Oncol Hematol. 2014; 91:1–8. [PubMed: 24457121]

4. Inaba H, Rubnitz JE, Coustan-Smith E, Li L, Furmanski BD, Mascara GP, et al. Phase I pharmacokinetic and pharmacodynamic study of the multikinase inhibitor sorafenib in combination with clofarabine and cytarabine in pediatric relapsed/refractory leukemia. J Clin Oncol. 2011; 29:3293–3300. [PubMed: 21768474]

5. Smolle E, Taucher V, Petru E, Haybaeck J. Targeted treatment of ovarian cancer--the multiple - kinase - inhibitor sorafenib as a potential option. Anticancer Res. 2014; 34:1519–1530. [PubMed: 24692678]

6. Drenberg CD, Baker SD, Sparreboom A. Integrating clinical pharmacology concepts in individualized therapy with tyrosine kinase inhibitors. Clin Pharmacol Ther. 2013; 93:215–219. [PubMed: 23419484]

7. Fukudo M, Ito T, Mizuno T, Shinsako K, Hatano E, Uemoto S, et al. Exposure-toxicity relationship of sorafenib in Japanese patients with renal cell carcinoma and hepatocellular carcinoma. Clin Pharmacokinet. 2014; 53:185–196. [PubMed: 24135988]

8. Ghassabian S, Rawling T, Zhou F, Doddareddy MR, Tattam BN, Hibbs DE, et al. Role of human CYP3A4 in the biotransformation of sorafenib to its major oxidized metabolites. Biochem Pharmacol. 2012; 84:215–223. [PubMed: 22513143]

9. Zimmerman EI, Roberts JL, Li L, Finkelstein D, Gibson AA, Chaudhry AS, et al. Ontogeny and sorafenib metabolism. Clin Cancer Res. 2012; 18:5788–5795. [PubMed: 22927483]

10. Peer CJ, Sissung TM, Kim A, Jain L, Woo S, Gardner ER, et al. Sorafenib is an inhibitor of UGT1A1 but is metabolized by UGT1A9: implications of genetic variants on pharmacokinetics and hyperbilirubinemia. Clin Cancer Res. 2012; 18:2099–2107. [PubMed: 22307138]

11. van Erp NP, Gelderblom H, Guchelaar HJ. Clinical pharmacokinetics of tyrosine kinase inhibitors. Cancer Treat Rev. 2009; 35:692–706. [PubMed: 19733976]

12. Roberts MS, Magnusson BM, Burczynski FJ, Weiss M. Enterohepatic circulation: physiological, pharmacokinetic and clinical implications. Clin Pharmacokinet. 2002; 41:751–790. [PubMed: 12162761]

13. Swift B, Nebot N, Lee JK, Han T, Proctor WR, Thakker DR, et al. Sorafenib hepatobiliary disposition: mechanisms of hepatic uptake and disposition of generated metabolites. Drug Metab Dispos. 2013; 41:1179–1186. [PubMed: 23482500]

14. Jain L, Woo S, Gardner ER, Dahut WL, Kohn EC, Kummar S, et al. Population pharmacokinetic analysis of sorafenib in patients with solid tumours. Br J Clin Pharmacol. 2011; 72:294–305. [PubMed: 21392074]

15. Zimmerman EI, Hu S, Roberts JL, Gibson AA, Orwick SJ, Li L, et al. Contribution of OATP1B1 and OATP1B3 to the disposition of sorafenib and sorafenib-glucuronide. Clin Cancer Res. 2013; 19:1458–1466. [PubMed: 23340295]

16. van de Steeg E, Stranecky V, Hartmannova H, Noskova L, Hrebicek M, Wagenaar E, et al. Complete OATP1B1 and OATP1B3 deficiency causes human Rotor syndrome by interrupting conjugated bilirubin reuptake into the liver. J Clin Invest. 2012; 122:519–528. [PubMed: 22232210]

17. van de Steeg E, Wagenaar E, van der Kruijssen CM, Burggraaff JE, de Waart DR, Elferink RP, et al. Organic anion transporting polypeptide 1a/1b-knockout mice provide insights into hepatic handling of bilirubin, bile acids, and drugs. J Clin Invest. 2010; 120:2942–2952. [PubMed: 20644253]

18. Iusuf D, van de Steeg E, Schinkel AH. Hepatocyte hopping of OATP1B substrates contributes to efficient hepatic detoxification. Clin Pharmacol Ther. 2012; 92:559–562. [PubMed: 23010652]

19. Choi YH, Yu AM. ABC transporters in multidrug resistance and pharmacokinetics, and strategies for drug development. Curr Pharm Des. 2014; 20:793–807. [PubMed: 23688078]

20. Li L, Zhao M, Navid F, Pratz K, Smith BD, Rudek MA, et al. Quantitation of sorafenib and its active metabolite sorafenib N-oxide in human plasma by liquid chromatography-tandem mass spectrometry. J Chromatogr B Analyt Technol Biomed Life Sci. 2010; 878:3033–3038.

21. Strumberg D, Richly H, Hilger RA, Schleucher N, Korfee S, Tewes M, et al. Phase I clinical and pharmacokinetic study of the Novel Raf kinase and vascular endothelial growth factor receptor inhibitor BAY 43-9006 in patients with advanced refractory solid tumors. J Clin Oncol. 2005; 23:965–972. [PubMed: 15613696]

22. Hing JP, Woolfrey SG, Greenslade D, Wright PM. Is mixed effects modeling or naive pooled data analysis preferred for the interpretation of single sample per subject toxicokinetic data? J Pharmacokinet Pharmacodynam. 2001; 28:193–210.

23. Liles JH, Flecknell PA. The influence of buprenorphine or bupivacaine on the post-operative effects of laparotomy and bile-duct ligation in rats. Lab Anim. 1993; 27:374–380. [PubMed: 8277712]

24. Emoto C, Yamazaki H, Yamasaki S, Shimada N, Nakajima M, Yokoi T. Characterization of cytochrome P450 enzymes involved in drug oxidations in mouse intestinal microsomes. Xenobiotica. 2000; 30:943–953. [PubMed: 11315103]

25. Hu C, Lancaster CS, Zuo Z, Hu S, Chen Z, Rubnitz JE, et al. Inhibition of OCTN2-mediated transport of carnitine by etoposide. Molecular Cancer Ther. 2012; 11:921–929.

26. Shibayama Y, Nakano K, Maeda H, Taguchi M, Ikeda R, Sugawara M, et al. Multidrug resistance protein 2 implicates anticancer drug-resistance to sorafenib. Biol Pharm Bull. 2011; 34:433–435. [PubMed: 21372398]

27. Cui Y, Konig J, Keppler D. Vectorial transport by double-transfected cells expressing the human uptake transporter SLC21A8 and the apical export pump ABCC2. Mol Pharmacol. 2001; 60:934–943. [PubMed: 11641421]

28. Keppler D. The roles of MRP2, MRP3, OATP1B1, and OATP1B3 in conjugated hyperbilirubinemia. Drug Metab Dispos. 2014; 42:561–565. [PubMed: 24459177]

29. Lathia C, Lettieri J, Cihon F, Gallentine M, Radtke M, Sundaresan P. Lack of effect of ketoconazole-mediated CYP3A inhibition on sorafenib clinical pharmacokinetics. Cancer Chemother Pharmacol. 2006; 57:685–692. [PubMed: 16133532]

30. Mani S, Boelsterli UA, Redinbo MR. Understanding and modulating mammalian-microbial communication for improved human health. Annu Rev Pharmacol Toxicol. 2014; 54:559–580. [PubMed: 24160697]

31. Kinouchi T, Kataoka K, Miyanishi K, Akimoto S, Ohnishi Y. Biological activities of the intestinal microflora in mice treated with antibiotics or untreated and the effects of the microflora on absorption and metabolic activation of orally administered glutathione conjugates of K-region epoxides of 1-nitropyrene. Carcinogenesis. 1993; 14:869–874. [PubMed: 8504479]

32. Nexavar package insert. 2012. see: www.berlex.bayerhealthcare.com

33. Tlemsani C, Huillard O, Arrondeau J, Boudou-Rouquette P, Cessot A, Blanchet B, et al. Effect of glucuronidation on transport and tissue accumulation of tyrosine kinase inhibitors: consequences for the clinical management of sorafenib and regorafenib. Expert Opin Drug Metab Toxicol. 2015; 25:1–10.
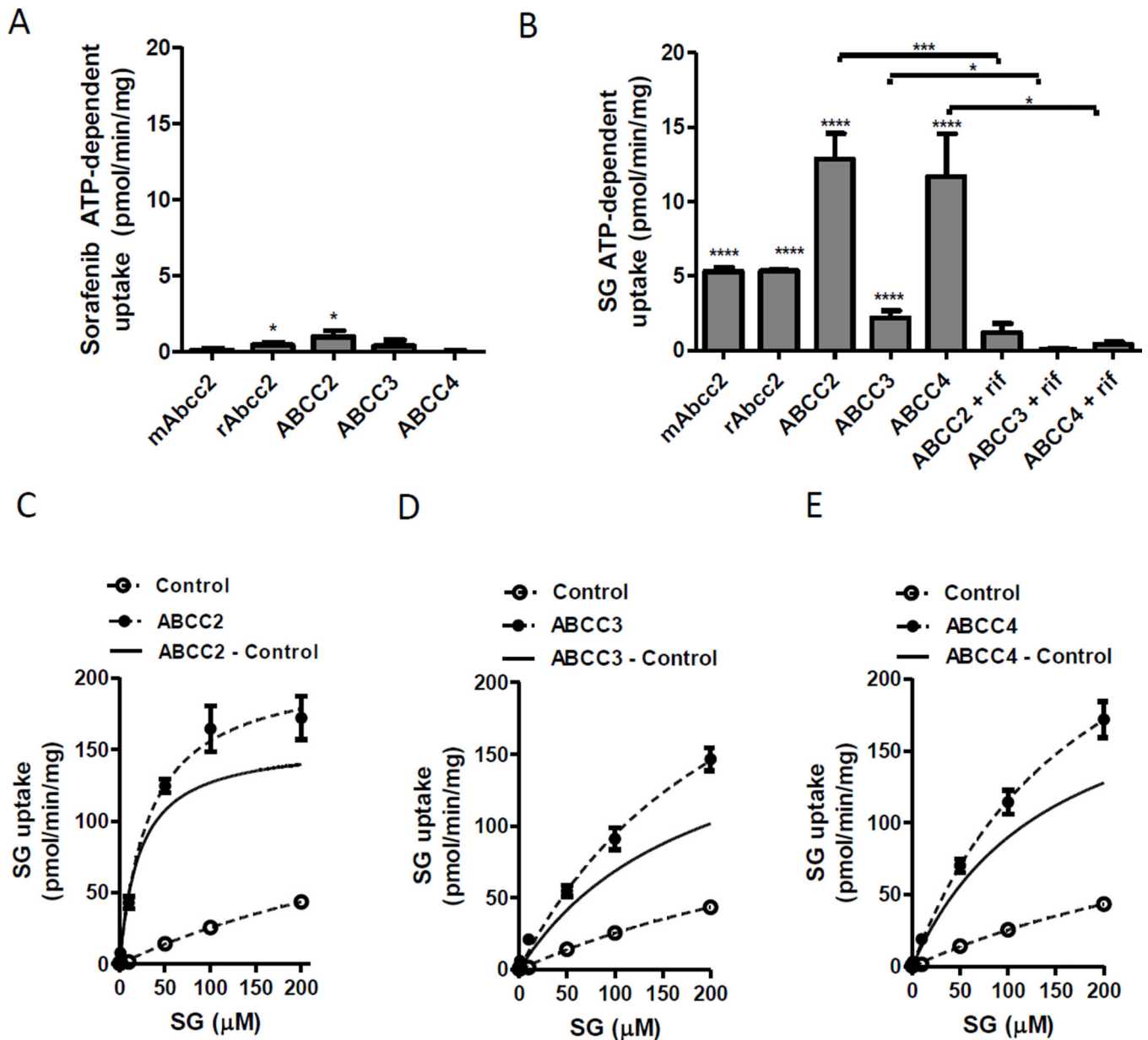
Figure 1.

Transport of sorafenib and SG by ABC transporters. Transport of (A) sorafenib (10 μM) or (B) SG (10 μM) in transporter-expressing inside-out vesicles using a 5-min incubation period in the presence or absence of ATP (4 mM) or rifampin (rif; 100 μM). Mouse and rat transporters are designated by the prefix "m" or "r", respectively. The human transporters are shown in capitals. Data represent the mean ± SE of difference between ATP- and AMP-dependent transport (both expressed in pmol/min/mg) after normalization for non-specific transport observed in control vesicles, from 3–4 independent experiments (3–18 replicates). Asterisks above bars indicate significant differences in uptake between vesicles expressing the indicated transporter and control vesicles: *, $P<0.05$; ***, $P<0.0005$; ****, $P<0.0001$. Square brackets: *, $P,0.05$ and **, $P<0.005$ for differences in uptake by ABCC2, ABCC3 or

ABCC4 with or without rifampin. (C) ABCC2-, (D) ABCC3-, or (E) ABCC4-expressing or control vesicles were incubated with increasing concentrations of SG for 5 minutes in the presence of ATP (4 mM).
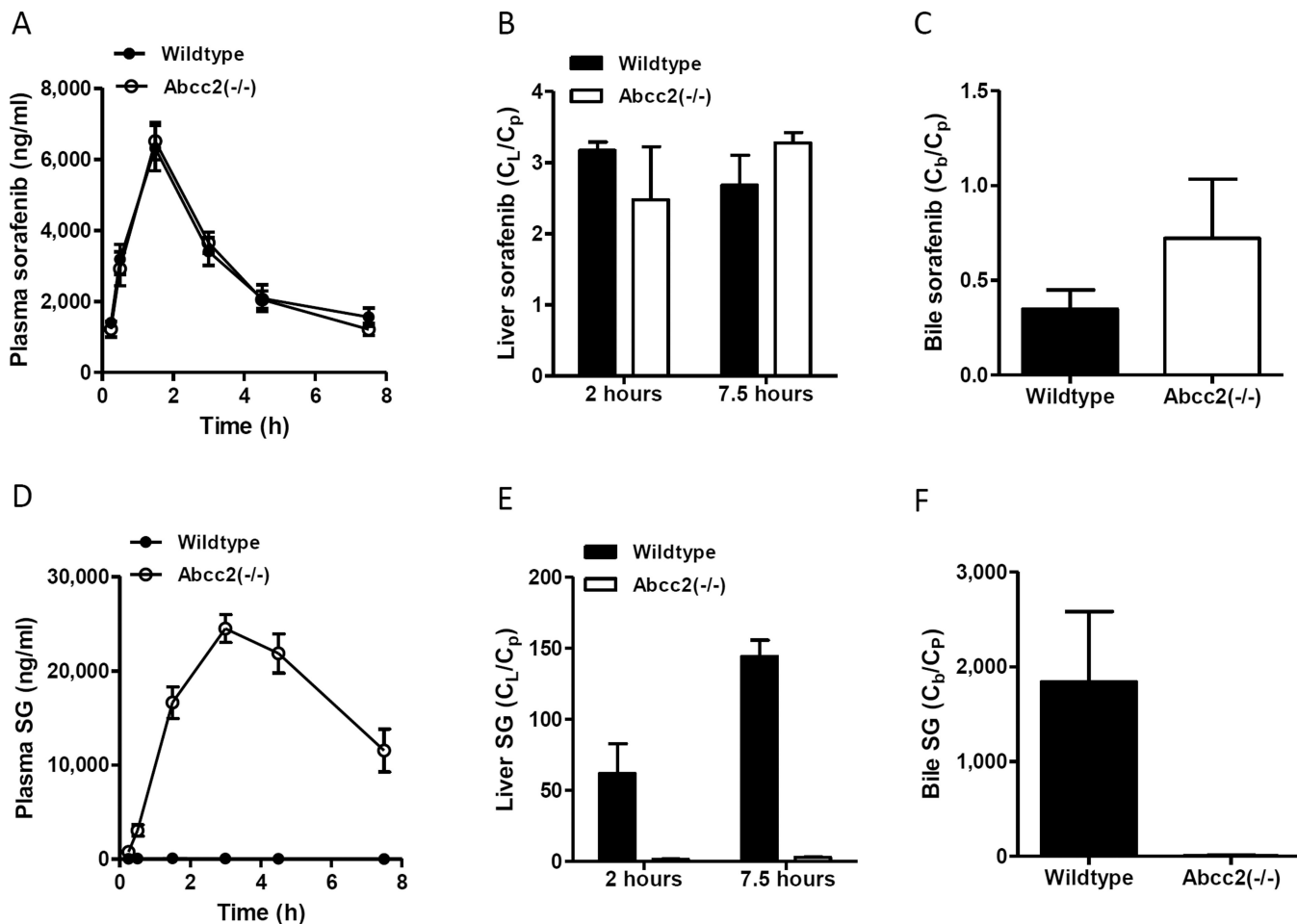
Figure 2.
Pharmacokinetics of sorafenib and SG in wildtype and Abcc2(−/−) mice. (A and D) Plasma
concentration-time profiles and (B and E) liver-to-plasma ratio of sorafenib and SG,
respectively, in female wildtype and Abcc2(−/−) mice. Sorafenib was administered orally at
a dose of 10 mg/kg. Livers were taken at 2 and 7.5 h after sorafenib administration (n = 4
per group). Concentrations in liver (C_L) were normalized to corresponding concentrations in
plasma (C_p). (C and F) Bile-to-plasma concentration ratios of sorafenib and SG,
respectively, in wildtype and Abcc2(−/−) mice. Sorafenib (10 mg/kg) was administered
orally 30 min before the start of bile collection (N=3 wildtype; N=2 Abcc2(−/−) mice). Bile
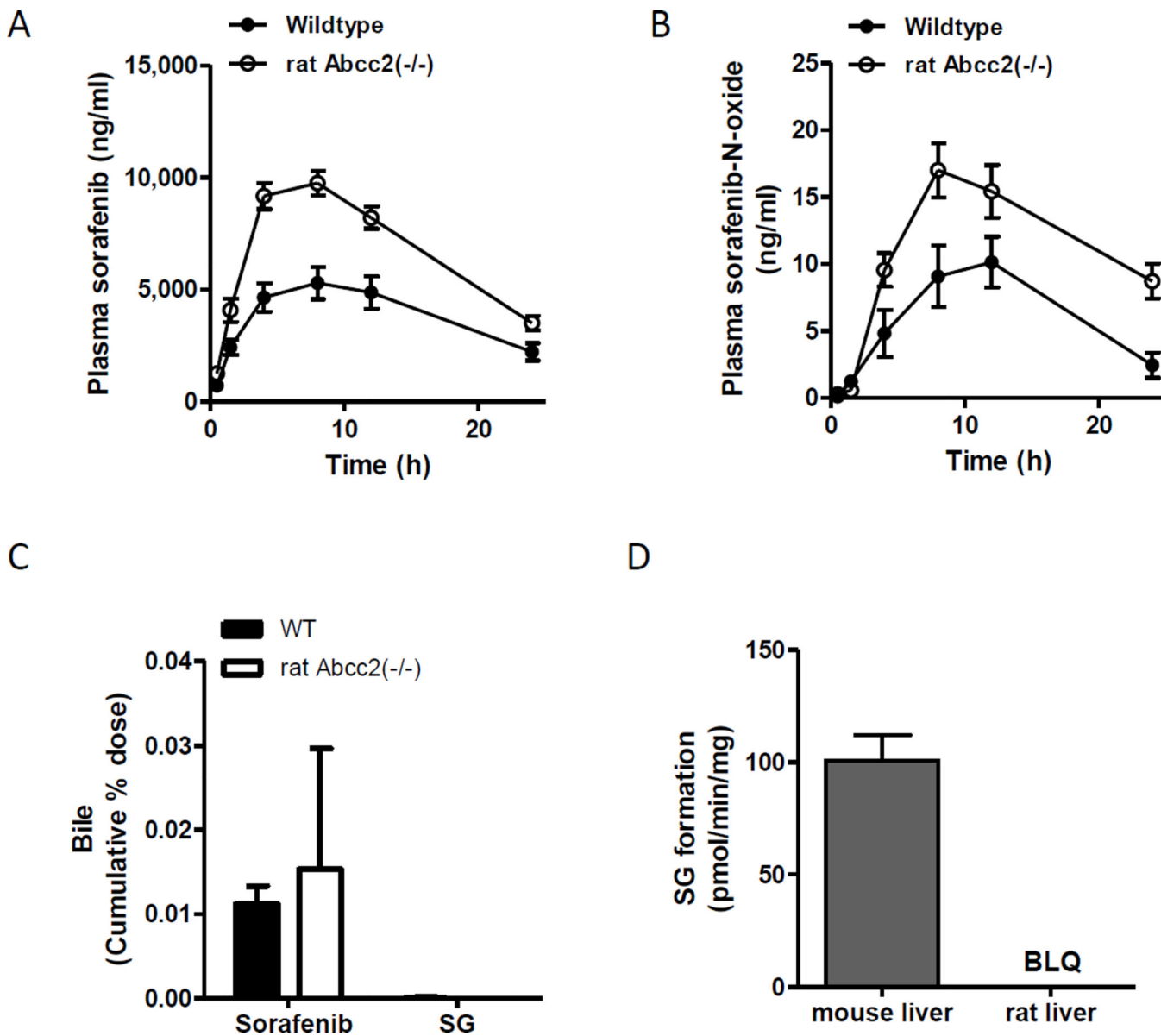was collected for 2 hours. Data represent the mean ± SE.

Figure 3.
Pharmacokinetics of sorafenib in wildtype and Abcc2(−/−) rats. Plasma concentration-time profiles of (A) sorafenib and (B) sorafenib N-oxide in wildtype and Abcc2(−/−) rats after oral administration of sorafenib at 10 mg/kg (n = 8 per group). SG concentrations were below the limit of quantitation (BLQ). Data represent the mean ± SE. (C) Biliary excretion of sorafenib and SG in wildtype and Abcc2(−/−) rats. Sorafenib (10 mg/kg) was administered orally 2 hours 25 min before bile collection (n = 2 per group). Bile was collected in 15-min fractions for 45 min. The results show collection at 2 hours 40 min after sorafenib administration (from 2 hours 25 min to 2 hours 40 min after sorafenib). (D) *Ex vivo* metabolism of sorafenib in liver microsomes of wildtype (WT) mice and rats. Liver microsomes (1 mg/ml) were incubated with 10 μM sorafenib for 60 min. Data represent the

mean ± SE from 1–2 independent experiments (3–6 replicates). BLQ, below the analytical assay limit of SG quantitation (<0.26 pmol/min/mg).
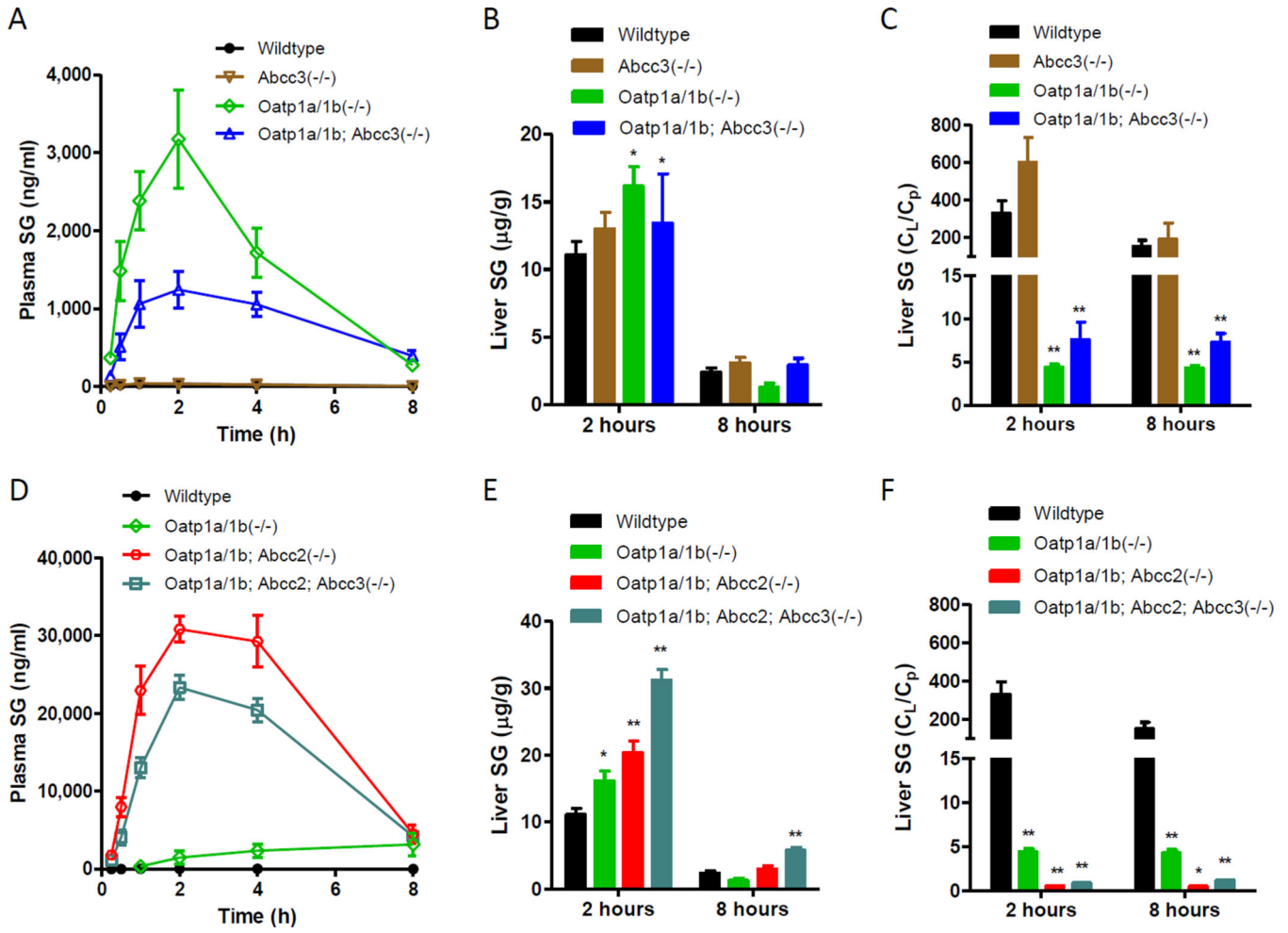
Figure 4.
Pharmacokinetics of SG in wildtype, Abcc3(−/−) mice, Oatp1a/1b(−/−), and combination
Abcc2(−/−) and Abcc3(−/−) mice. Concentration-time profiles of SG in plasma (A, D), liver
(B, E), and liver-to-plasma ratios (C, F) in wildtype and transporter knockout mice.
Sorafenib 10 mg/kg was administered orally (n   4 per group). Data represent the mean ±
SE. Asterisks indicate a significant difference in SG liver concentrations and liver to plasma
concentration ratios between transporter knockout and wildtype mice: *, $P<0.05$; **,
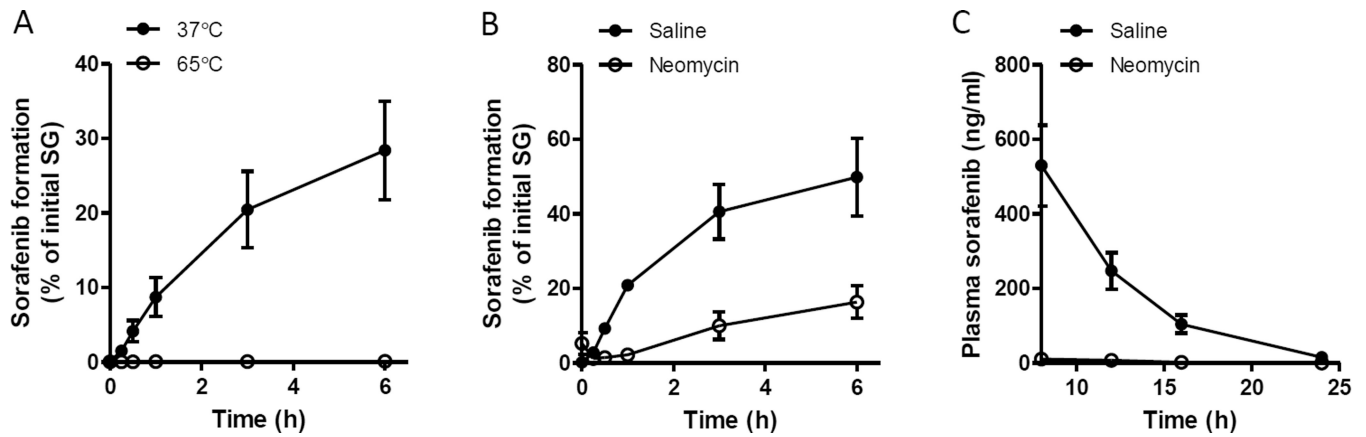$P<0.005$.

Figure 5.

Sorafenib formation from SG by mouse intestinal contents. (A) Formation of sorafenib upon *ex vivo* incubation of FVB mouse cecal contents with SG (2 μM) with or without heat pre-treatment (65°C) or (B) after treatment of mice with saline or oral neomycin 200 mg/kg given twice daily for 5 days (n   4 per group). Data were normalized to SG concentration at t=0 and represent the mean ± SE. (C) Sorafenib plasma concentrations in mice pre-treated with oral neomycin (200 mg/kg) given twice daily for 5 days. On the day of blood sample collection, SG (10 mg/kg) was administered orally. Sorafenib was not detected in plasma until 8 hours after administration of SG. All animals were female FVB mice. Data represent the mean ± SE.
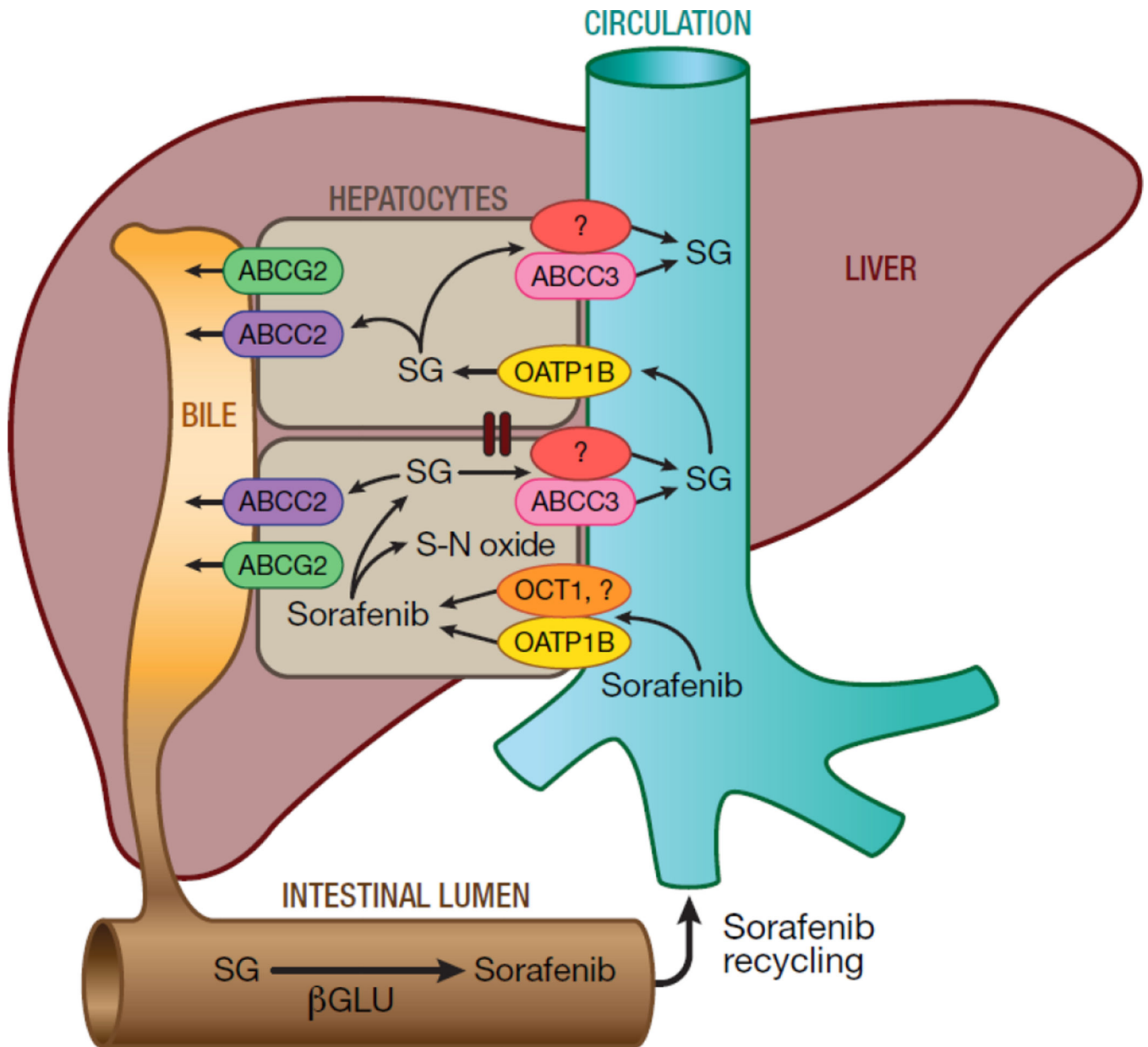
Figure 6.
Hepatocyte hopping and recirculation of SG. After oral administration, sorafenib enters the hepatocytes by incompletely defined transporters mechanisms, including OATP1B-type carriers and OCT1, and undergoes CYP3A4 mediated metabolism to sorafenib-N-oxide (s-N-oxide) and conjugation by UGT1A9 to form SG. After conjugation, SG is extensively secreted into the bile by a process that is mainly mediated by ABCC2. Under physiological conditions, a fraction of the intracellular SG is secreted by ABCC3 and at least one other transporter back to the blood, from where it can be taken up again into downstream hepatocytes via OATP1B1-type carriers (Oatp1a and Oatp1b in mice). This secretion-and-reuptake loop may prevent the saturation of ABCC2-mediated biliary excretion in the upstream hepatocytes, thereby ensuring efficient biliary elimination and hepatocyte

detoxification. Once secreted into bile, SG enters the intestinal lumen where it serves as a substrate for as yet unknown bacterial β-glucuronidases (β-GLU) that produce sorafenib, which is subsequently undergoing intestinal absorption and re-enters the systemic circulation.